THE JOURNAL OF PHYSICAL CHEMISTRY Letters

pubs.acs.org/JPCL

First-Principles-Based Dispersion Augmented Density Functional Theory: From Molecules to Crystals

Yi Liu* and William A. Goddard, III*

Materials and Process Simulation Center, California Institute of Technology, Pasadena, California 91125

ABSTRACT Standard implementations of density functional theory (DFT) describe well strongly bound molecules and solids but fail to describe long-range van der Waals attractions. We propose here first-principles-based augmentation to DFT that leads to the proper long-range $1/R^6$ attraction of the London dispersion while leading to low gradients (small forces) at normal valence distances so that it preserves the accurate geometries and thermochemistry of standard DFT methods. The DFT-low gradient (DFT-*lg*) formula differs from previous DFT-D methods by using a purely attractive dispersion correction while not affecting valence bond distances. We demonstrate here that the DFT-*lg* model leads to good descriptions for graphite, benzene, naphthalene, and anthracene crystals, using just three parameters fitted to reproduce the full potential curves of high-level ab initio quantum mechanics [CCSD(T)] on gas-phase benzene dimers. The additional computational costs for this DFT-*lg* formalism are negligible.

SECTION Molecular Structure, Quantum Chemistry, General Theory

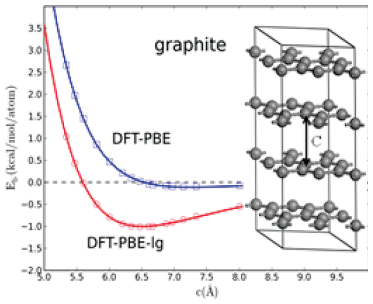

London dispersive interactions[1] (van der Waals attraction) play an essential role in biological systems, molecular electronics, energetic materials, and molecular crystals. Current implementations of density functional theory[2] (DFT) describe well the intramolecular geometries and energies for such systems but fail to treat London dispersive interactions[3] important in intermolecular interactions. A simple example is that graphite at the PBE level of DFT[4] predicts an infinite interlayer separation. Similar demonstrations have been published for systems ranging from weakly bound complexes[5] to π-stacking of DNA pairs.[6]

For finite molecules, ab initio quantum mechanics (QM) at the CCSD(T) (coupled cluster singles and doubles plus perturbative triples) level takes into account the simultaneous single excitations of electron pairs on different centers at the heart of London dispersion, leading to an accurate treatment of dispersion for molecular complexes such as benzene dimers.[7] However, the CCSD(T) method scales as N^7, making it impractical for calculations on crystals or biological macromolecules such as proteins and DNA.

We propose here a simple first-principles-based augmentation to DFT that

- leads to a proper $1/R^6$ London dispersion interaction at sufficiently long distances that the molecular orbitals do not overlap
- maintains small forces (low gradients) at short distances so that it does not affect valence geometries and cohesive energies of covalent molecules, which are already described well with widely used DFT methods
- introduces only a single set of parameters for each pairwise interaction type (C−C, C−H, and H−H), all derived from highly accurate CCSD(T) ab initio calculations on model complexes and then used to correct the interactions of large molecular complexes and crystals

We adopt the DFT-low gradient (DFT-*lg*) model of eq 1

$$E_{\text{DFT-lg}} = E_{\text{DFT}} + D_{lg}$$

$$\text{where} \quad D_{lg} = -\sum_{ij,\, i<j}^{N} \frac{C_{lg,\,ij}}{r_{ij}^6 + b_{lg} R_{0ij}^6} \qquad (1)$$

Here, $C_{lg,ij}$ is the parameter measuring the strength of the missing dispersive interaction between atoms i and j separated by r_{ij}. To determine the scale at which this dispersion form is appropriate, we take R_{0ij} as the typical equilibrium vdW distance between atoms i and j. Here, we adopt the vdW radii from the UFF force field[8] since it is defined for all atoms up through Lr (element 103). The scaling parameter $b_{lg} = 1$ is fixed here but could be adjusted if a system requires shifting the location of the maximum gradient (this might occur because the vdW radii of many elements remain uncertain). The D_{lg} dispersion function is purely attractive (increasing monotonically with distance) but becomes constant at distances much shorter than the standard vdW radii; therefore, it should not affect valence geometries or energies. We consider this to be an advantage over previously suggested forms[9−13] in which the correction force is attractive at the largest R but repulsive at smaller R (see Figure 1 and Figure S1 of Supporting Information [SI]), which we consider nonphysical. Thus

Received Date: May 12, 2010
Accepted Date: August 5, 2010
Published on Web Date: August 11, 2010

DOI: 10.1021/jz100615g | *J. Phys. Chem. Lett.* **2010**, *1*, 2550–2555

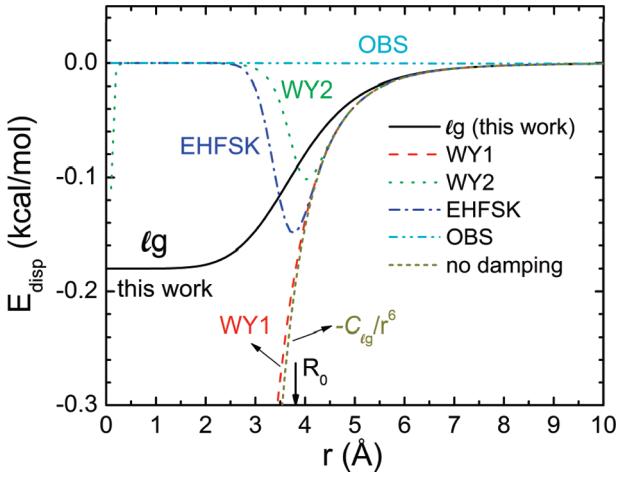

Figure 1. Dispersion correction (E_{disp}) developed in this work (denoted as *lg*) for interactions of two carbon atoms compared with other methods (WY1,[9] WY2,[9] EHFSK,[11] and OBS[12]). The same C−C equilibrium bond distance R_0 = 3.851 Å and C_{lg} = 586.8 kcal/mol Å^6 are used for all curves. $E_{disp} = -C_{lg}/r^6$ without damping is also plotted.

DFT-*lg* is distinctly different from previous DFT-D methods[9−13] that use a multiplier as a damping function. Since DFT-*lg* leads to small forces for intramolecular distances, it should have little effect on the cohesive energies (thermochemistry) used in defining the parameters of current DFT methods. It would affect the energies of molecular complexes used in the M06 and X3LYP flavors of DFT but not others. Thus, the *lg* correction does not require a modification in the standard DFT parameters.

In this work, we show that the DFT-*lg* model with just three parameters (namely, $C_{lg,ij}$, where *ij* = C−C, C−H, and H−H) corrects the PBE[14] or B3LYP[15] levels of DFT to reproduce the full potential curves of high-level ab initio quantum mechanics [CCSD(T)] for the benzene dimers. Moreover, the parameters obtained from the benzene dimers lead to good structures and energies for graphite, benzene, naphthalene, and anthracene crystals without refitting. This transferability validates the DFT-*lg* model for describing London dispersion of molecules and solids.

Various strategies have been suggested for overcoming the dispersion problem in DFT:

(1) Go beyond the conventional DFT Kohn−Sham formula[2] to include excitations to the virtual orbitals by solving the time-dependent DFT (TD-DFT) equation[16] or by reformulating the DFT Hamiltonian (e.g., XYG3[17]).

(2) Use the conventional DFT framework, but modify the exchange-correlation functionals (E_{xc}) to account for the long-range correlation description implicitly. The hope is that the new functional would improve the overall performance, including the vdW description. Examples of this approach are M06 and X3LYP.[18]

(3) Incorporate a dispersion term explicitly through ad hoc augmentation. One can accomplish this by solving a modified Hamiltonian quantum mechanically[19] or by adding an empirical classical term evaluated separately.[9−13]

The DFT-*lg* method belongs to category (3) but is first-principles-based since all the parameters are determined from high-level QM. DFT-*lg* involves negligible extra computational cost, making it practical for all systems being treated at the PBE or B3LYP levels of DFT.

Becke and Johnson (BJ)[18c] built a somewhat similar damping strategy into their exact-exchange-based energy functional. The BJ approach is essentially different from the ad hoc DFT-D methods (category 3 described above and including DFT-*lg*) that provide a correction to the final energy from DFT. Instead, BJ calculates dispersion parameters (C_6−C_{10} etc.) from the position-dependent dipole moment of the exchange hole, which is nonempirical but rather expensive. The additional term, the effective vdW distance, R_{0ij}, in the denominator of the BJ form is a function of C_6−C_{10} parameters plus two atom-independent empirical parameters determined by least-squares fitting to vdW calibration data. On the other hand, we use a standard set of equilibrium vdW distances taken from UFF. We also add a scaling parameter b_{lg} to provide further flexibility, but we have not needed this flexibility yet. Thus, DFT-*lg* does not modify the DFT functional as BJ does.

The benzene dimer is the simplest prototype system for studying aromatic π−π interactions. Benzene dimers have several important configurations, T-shaped (T), sandwich (S), and parallel-displaced (PD) configurations (see inserts of Figure 2). High-level ab initio CCSD(T) calculations[7,20] were carried out using an aug-cc-pVQZ* basis set with counterpoise (CP) corrections. These calculations show that the T and PD configurations have a comparable binding energy of ∼2.9 kcal/mol, but the S configuration is less stable by ∼30 % (Figure 2 and S2, SI).

We calculated the binding energies of benzene dimers for all three configurations using DFT PBE with a 6-311G**++ basis set and fine grids.[21] Comparing the PBE and the CCSD(T) results shows that PBE finds no binding for the S and PD structures (Figure 2) and accounts for only 42 % of the binding energy for the T structure, leading to the equilibrium distance being too long by 0.3 Å (6 %).

Despite the poor description of benzene dimers with PBE, PBE-*lg* reproduces well the full CCSD(T) potential curves for all three configurations over the wide range of separations in Figure 2. This good agreement demonstrates that the DFT-*lg* formalism is adequate for describing London dispersion since these benzene configurations exhibit distinct binding characteristics, including dispersive and electrostatic interactions. With only three C_{lg} dispersion parameters, C−C, H−H, and C−H (Table S2, SI), we fit the dispersion corrections for all three configurations as a function of distance. This suggests that these dispersion parameters may be applicable to other conformations found in crystal packing or dynamics. To optimize parameters, we used Computational Materials Design Facility (CMDF) software[13,22] that implements full parameter gradients. Thus, we consider that DFT-*lg* provides an extension of the accuracy of CCSD(T) to the practical description of the dynamics of large interacting vdW complexes.

We use the same procedure to obtain three B3LYP-*lg* parameters that correct the B3LYP level of DFT (Table S2 of SI). The B3LYP-*lg* model also reproduces the CCSD(T) results

DOI: 10.1021/jz100615g | J. Phys. Chem. Lett. 2010, 1, 2550–2555

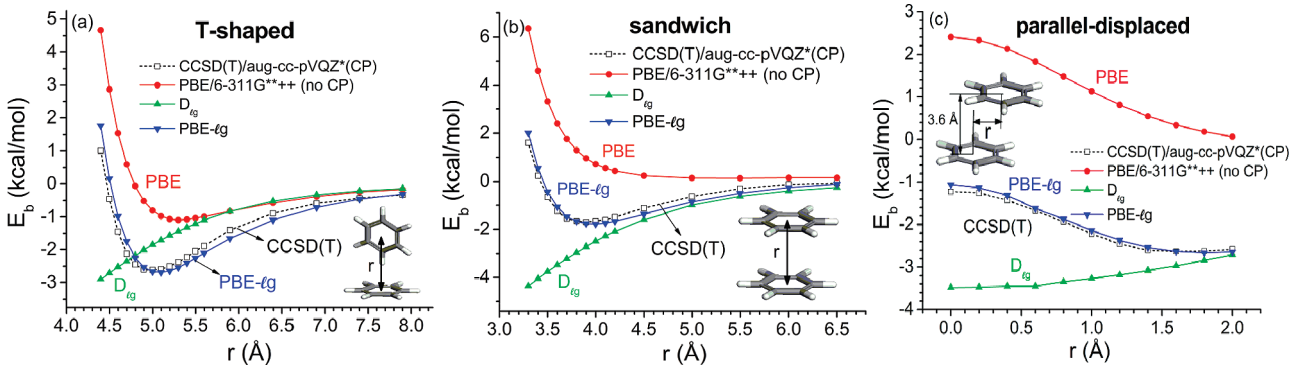

Figure 2. Binding energy (E_b) of benzene dimers as a function of distance calculated using the pure PBE and the dispersion-corrected method PBE-*lg* for (a) T-shaped, (b) sandwich, and (c) parallel-displaced configurations. The C_{lg} parameters in the DFT-*lg* model (eq 1) are C−C, 586.8113; H−H, 31.1372; and C−H, 8.6912 kcal/mol·Å^6 (Table S2, SI).

Table 1. Equilibrium c_0 Lattice Parameters, Interlayer Binding Energies (BE), and Elastic Constant C_{33} of Graphite Calculated by the DFT-*lg* Method, Compared with Quantum Monte Carlo (QMC), DFT Calculations, and Experiments[a]

	c_0 (Å)			BE (kcal/mol/atom)		C_{33} (GPa)		
	0 K	0 K + ZPE	300 K + ZPE	0 K	300 K + ZPE	0 K	0 K + ZPE	300 K + ZPE
PBE DFT[4]	8.49	8.5102(27.5%)[b]	8.5244(27.1%)[c]	0.06	0.058[d]	2.4	2.37(−94.2%)[e]	2.41 (−93.4%)[f]
nonlocal DFT[32]	7.0	7.0167(5.2%)[b]	7.0284(4.8%)[c]	0.78	0.76[d]	33	32.59(−19.9%)[e]	33.20 (−9.0%)[f]
QMC[31]	6.8527	6.8690(3.0%)[b]	6.8805(2.6%)[c]	1.38	1.34[d]	36.6	36.15(−11.2%)[e]	36.83 (0.9%)[f]
DFT-*lg*	6.5080	6.5235(−2.2%)[b]	6.5344(−2.6%)[c]	1.00	0.97[d]	38.69	38.21(−6.1%)[e]	38.93(6.7%)[f]
experiments	6.6562[b]	6.6721[23]	6.7090[24]	1.24[d]	1.20 ± 0.12[30]	41.2[e]	40.7 ± 1.1 (unpublished)	36.5 ± 1[26]
				1.02[d]	0.99 ± 0.12[29]			
				0.84[d]	0.81 ± 0.23[28]			

[a] The DREIDING force field[27] was used to calculate the corrections of zero-point energy (ZPE) and lattice vibrations (VIB) at 300 K. [b] ZPE correction: 0.24%. [c] ZPE and VIB corrections: 0.41%. [d] ZPE and VIB corrections: 3.0%. [e] ZPE correction: 1.2%. [f] ZPE and VIB corrections: 0.6%.

well for all three configurations (Figure S3, SI), despite the B3LYP description of the benzene dimers being even worse than PBE. Similarly, one could define HF-*lg* parameters to go from simple Hartree−Fock to full dispersion correction (see the application to inert gas dimers in the SI).

Graphite crystals provide an excellent benchmark system for validating the DFT-*lg* dispersion model for solids since London dispersion is responsible for the binding between graphene layers, determining the interlayer separation (c/2). Using all-electron projected augmented wave (PAW) potentials, Ooi et al.[4] showed that PBE failed completely to describe interlayer bonding in graphite, leading to infinite separation and no binding. Recent PBE calculations[4] with ultrasoft (US) pseudopotentials by Mounet et al. led to an extremely weak attraction (presumably due to the US pseudopotential) with an optimal c of graphite of 8.49 Å, which is 1.8 Å or 27% larger than the experimental c = 6.6721 Å (extrapolated to 0 K).[23,24] They obtained a PBE interlayer binding energy[4] of 0.06 kcal/mol, only 1/17 of the experimental values (ranging from 0.8 to 1.2 kcal/mol[28−30]).

We carried out energy minimizations on 2 × 2 × 2 graphite supercells using DFT PBE[25] with norm-conserving pseudopotentials and a local contracted-Gaussian basis set. These PBE calculations lead to c = 7.14 Å (14% larger than experiment) and an interlayer binding energy of 0.10 kcal/mol (10% of experiment). Using the same C−C_{lg} parameter from fitting to the benzene dimers, PBE-*lg* leads to c = 6.5235 Å, 2.2% smaller than experiment. PBE-*lg* predicts a sheet−sheet elastic constant of C_{33} = 38.21 GPa, 6.1% smaller than experiment, 40.7 GPa at 0 K[26] (Table 1). PBE-*lg* leads to an interlayer binding energy (BE) of 0.97 kcal/mol, which is consistent with the three experimental values of 0.81 ± 0.23,[28] 0.99 ± 0.12,[29] and 1.20 ± 0.12[30] kcal/mol.

Recent quantum Monte Carlo (QMC) calculations for graphite[31] led to c = 6.853 Å at 0 K (0.33 Å or 5% larger than experiment) and BE = 1.38 ± 0.23 kcal/mol (~20−60% larger than experiment). Although QMC is not practical to use sufficiently large supercells to obtain convergence, even for graphite, our PBE-*lg* values are consistent with the QMC results, given the current level of convergence for QMC.

Nonlocal effects were recently incorporated into DFT to account for dispersion,[32] leading to c = 7.0 Å (0.5 Å too long) and BE = 0.76 kcal/mol for graphite.[32]

At negligible extra computational cost, PBE-*lg* provides more accurate results than the current levels of QMC and nonlocal DFT methods in predicting equilibrium interlayer separation, interlayer binding energy, and C_{33} elastic constant of graphite (Table 1). Thus, PBE-*lg* results could serve as a benchmark for studying dispersive interactions in solids.

DOI: 10.1021/jz100615g | J. Phys. Chem. Lett. 2010, 1, 2550–2555

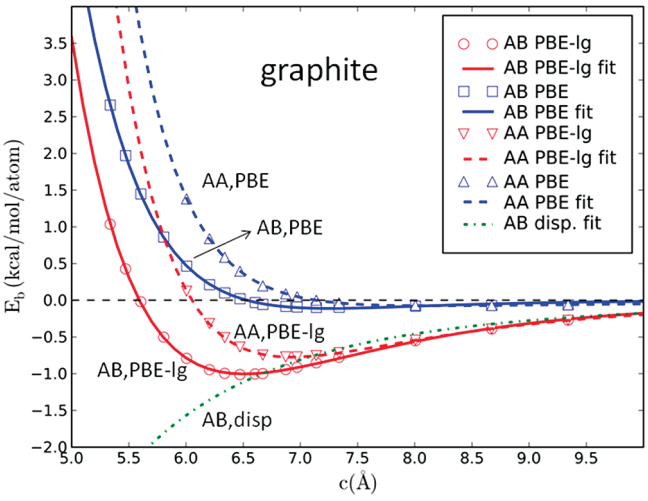

Figure 3. Binding energies (E_b) as a function of c lattice parameters of graphite crystals with AB and AA stacking at 0 K. The solid lines represent least-squares fits to the PBE-*lg* results, while the dashed lines are for PBE. $F = 6$ is fixed in fitting PBE-*lg* for AB-stacking graphite; full optimization would lead to $F = 6.0580$. The fitting function is $E_b(c) = A \exp[B(c - c_0)] + D/(c/c_0)^F$. The parameters for AB,PBE-*lg* are $A = 1.3914$, $B = -1.5870$, $c_0 = 6.5080$, $D = -2.3957$, and $F = 6.0000$; those for AB,PBE are $A = 0.2443$, $B = -1.8761$, $c_0 = 7.2560$, $D = -0.3558$, and $F = 9.3446$; for AA, PBE-*lg*, they are $A = 0.5165$, $B = -1.8394$, $c_0 = 6.9211$, $D = -1.2912$, and $F = 5.0923$; the values for AA,PBE are $A = 0.0144$, $B = -2.2106$, $c_0 = 8.1370$, $D = -0.0903$, and $F = 2.8567$. The fitting parameters are also listed in Table S4 (SI). The dot−dash line represents the fitted *lg* dispersive interaction for AB-stacking graphite. The fitting function is $E_{disp}(c) = G/(c/c_0)^H$, where $c_0 = 6.5080$, $G = -1.1091$, and $H = 4.2790$.

PBE-*lg* predicts eclipsed graphite (AA stacking) to be 0.23 kcal/mol less stable than AB stacking (Figure 3), with an interlayer separation of 3.4606 Å, 6% larger than the AB-stacking graphite.

Benzene crystal structures are known at temperatures down to 15 K and at pressures up to 1.1 GPa from X-ray and neutron scattering spectroscopy (Figure S5, SI). From these data, we derived an "experimental" zero-temperature equation of state (EOS) (Figure S6 of SI). PBE overestimates the volume at 0 K by 35.0%, a direct consequence of the missing dispersive interactions. At the experimental 0 K geometry, PBE leads to a pressure of 1.43 GPa (Figure 4).

Using the PBE-*lg* dispersion parameters for the benzene dimers, the PBE-*lg* EOS agrees well with the corrected experimental EOS at 0 K (Figure 4). At ambient pressure, the PBE-*lg* volume is 2.8% larger than that from experiment, 13 times better than the 35.0% expansion predicted by PBE alone (Table S8, SI). The PBE-*lg* pressure at the experimental equilibrium volume is 0.11 GPa, 13 times better than PBE. This suggests good transferability of molecular cluster results to molecular crystals.

The experimental heat of sublimation ($\Delta_{sub}H$) for benzene is 10.612 kcal/mol at 190 K (Table S9 of SI). Correcting for the specific heat and the zero-point energy[27] leads to a value of 11.295 kcal/mol at 0 K. This can be compared to 0.913 kcal/mol for PBE (92% error) and 6.762 kcal/mol for PBE-*lg* (S9), 40% error. This may indicate that we need to allow optimization of the b_{lg} parameter. Thus, the *lg* dispersion correction

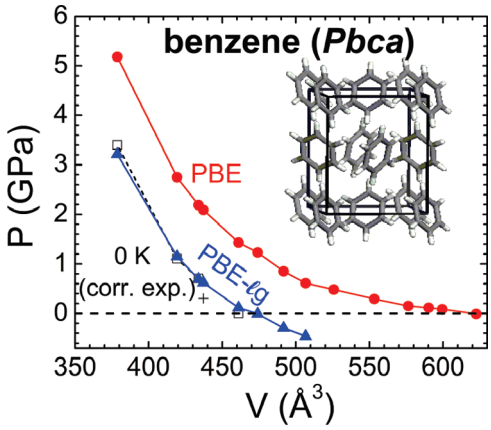

Figure 4. EOS of benzene crystal (orthorhombic phase I) calculated using the PBE and PBE-*lg* methods, compared with the corrected experimental EOS at 0 K (dashed line).

improves significantly both the structure and the binding energy of the crystal.

To examine the transferability of the benzene-based dispersion correction to other molecules, we studied the naphthalene and anthracene polycyclic aromatic hydrocarbon (PAH) crystals. On the basis of the EOS at 298 K and various pressures (Figures S10 and S11 of SI), we derived a zero-temperature EOS of the naphthalene crystal to serve as a reference for validation (Figures S12 and S13 of SI). We calculated pressures at various volumes using PBE and PBE-*lg*. For naphthalene, the PBE equilibrium volume is 24.7% too large, whereas the PBE-*lg* volume is 3.4% too small, a factor of 7 improvement (Table S8, SI). At the experimental geometry, PBE leads to a total pressure of 1.24 GPa, compared to −0.31 GPa from PBE-*lg*. The experimental $\Delta_{sub}H$ for naphthalene is 17.208 kcal/mol. Correcting for zero-point energy and specific heat[27] leads to 20.095 kcal/mol at 0 K. This can be compared to the PBE value of 2.043 kcal/mol and the PBE-*lg* value of 11.335 kcal/mol (Table S9, SI).

For the anthracene crystal, PBE predicts an equilibrium volume that is 28.6% larger than that of experiment (extrapolated to 0 K), whereas the PBE-*lg* value is too small by 2.2% (Table S8, SI). At the experimental 0 K structure, PBE leads to a pressure of 1.39 GPa, whereas PBE-*lg* leads to −0.28 GPa (Table S8, SI). The experimental $\Delta_{sub}H$ for anthracene is 23.423 kcal/mol. Correcting for zero-point energy and specific heat[27] leads to 27.042 kcal/mol at 0 K. This can be compared to the PBE value of −0.286 kcal/mol and the PBE-*lg* value of 12.329 kcal/mol (Table S9, SI).

The calculated binding energies as a function of volume for benzene (Figure S14, SI) and naphthalene (Figure S15, SI) crystals confirm the dramatic improvement with DFT-*lg*.

DFT-*lg* also leads to good descriptions of the vdW equilibrium distances and binding energies for diatomic rare gas molecules from He−He to Xe−Xe (Figure S16 and Table S17 of SI).

The DFT-*lg* method should lead to more reliable ab initio molecular dynamics simulations since the distinct low gradient feature eliminates artificial repulsive dispersion forces at smaller distances in most current DFT-D methods. Recently,

DOI: 10.1021/jz100615g | J. Phys. Chem. Lett. 2010, 1, 2550–2555

we developed the XYG3 DFT method[17] that includes double excitations to Kohn–Sham virtual orbitals, leading to excellent accuracy for describing the potential surfaces of molecular complexes and reactions, including those dominated by the vdW dispersion. However, XYG3 is far more costly than PBE or B3LYP. We propose that the DFT-*lg* method might provide a pragmatic strategy to describe dispersion in large-scale systems followed by single-point XYG3 calculations at critical points.

SUPPORTING INFORMATION AVAILABLE The full set of dispersion correction (*lg*) parameters for PBE and B3LYP are included. This material is available free of charge via the Internet at http://pubs.acs.org.

AUTHOR INFORMATION

Corresponding Author:

*To whom correspondence should be addressed. E-mail: yi@wag.caltech.edu; wag@wag.caltech.edu.

ACKNOWLEDGMENT This research received support from ARO (W911NF-05-1-0345; W911NF-08-1-0124, Ralph Anthenien), ONR (N00014-05-1-0778, Cliff Bedford), and Los Alamos National Laboratory (LANL65287, Ed Kober).

REFERENCES

(1) (a) London, F. Zur Theorie und Systematik der Molekularkräfte. *Z. Phys.* **1930,** *63*, 245. (b) London, F. The General Theory of Molecular Forces. *Trans. Faraday Soc.* **1937,** *33*, 8–26.

(2) (a) Hohenberg, P.; Kohn, W. Inhomogeneous Electron Gas. *Phys. Rev. B* **1964,** *136*, B864. (b) Kohn, W.; Sham, L. J. Self-consistent Equations Including Exchange and Correlation Effects. *Phys. Rev.* **1965,** *140*, 1133.

(3) Koch, W.; Holthausen, M. C. *A Chemist's Guide to Density Functional Theory*; Wiley-VCH: Weinheim, Germany, 2001.

(4) (a) Mounet, N.; Marzari, N. First-Principles Determination of the Structural, Vibrational and Thermodynamic Properties of Diamond, Graphite, and Derivatives. *Phys. Rev. B* **2005,** *71*, 205214. (b) Ooi, N.; Rairkar, A.; Adams, J. B. Density Functional Study of Graphite Bulk and Surface Properties. *Carbon* **2006,** *44*, 231–242.

(5) (a) Merkle, R.; Savin, A.; Preuss, H. Singly Ionized 1st-row Dimers and Hydrides Calculated with the Fully Numerical Density-functional Program NUMOL. *J. Chem. Phys.* **1992,** *97*, 9216–9221. (b) Kristyan, S.; Pulay, P. Can (Semi)Local Density-Functional Theory Account for the London Dispersion Forces. *Chem. Phys. Lett.* **1994,** *229*, 175–180. (c) Perezjorda, J. M.; Becke, A. D.; Density-functional, A Study of van-der-Waals Forces — Rare-Gas Diatomics. *Chem. Phys. Lett.* **1995,** *233*, 134–137. (d) Hobza, P.; Sponer, J.; Reschel, T. Density-functional Theory and Molecular Clusters. *J. Comput. Chem.* **1995,** *16*, 1315–1325. (e) Meijer, E. J.; Sprik, M. A Density-Functional Study of the Intermolecular Interactions of Benzene. *J. Chem. Phys.* **1996,** *105*, 8684–8689. (f) Tkatchenko, A.; von Lilienfeld, O. A. Popular Kohn–Sham Density Functionals Strongly Overestimate Many-Body Interactions in van der Waals Systems. *Phys. Rev. B* **2008,** *78*, 45116.

(6) (a) Waller, M. P.; Robertazzi, A.; Platts, J. A.; Hibbs, D. E.; Williams, P. A. Hybrid Density Functional Theory for π-Stacking Interactions: Application to Benzenes, Pyridines, and DNA Bases. *J. Comput. Chem.* **2006,** *27*, 491–504. (b) Zhao, Y.; Truhlar, D. G. Density Functionals for Noncovalent Interaction Energies of Biological Importance. *J. Chem. Theory Comput.* **2007,** *3*, 289–300.

(7) Sinnokrot, M. O.; Sherrill, C. D. Highly Accurate Coupled Cluster Potential Energy Curves for the Benzene Dimer: Sandwich, T-shaped, and Parallel-Displaced Configurations. *J. Phys. Chem. A* **2004,** *108*, 10200–10207.

(8) Rappe, A. K.; Casewit, C. J.; Colwell, K. S.; Goddard, W. A.; Skiff, W. M. UFF, A Full Periodic-Table Force-Field for Molecular Mechanics and Molecular-Dynamics Simulations. *J. Am. Chem. Soc.* **1992,** *114*, 10024–10035.

(9) (a) Wu, Q.; Yang, W. T. Empirical Correction to Density Functional Theory for van der Waals Interactions. *J. Chem. Phys.* **2002,** *116*, 515–524. (b) Ahlrichs, R.; Penco, R.; Scoles, G. Intermolecular Forces in Simple Systems. *Chem. Phys.* **1977,** *19*, 119–130. (c) Neumann, M.; Perrin, M. Energy Ranking of Molecular Crystals Using Density Functional Theory Calculations and an Empirical van der Waals Correction. *J. Phys. Chem. B* **2005,** *109*, 15531–15541. (d) Gonzalez, C.; Lim, E. C. Evaluation of the Hartree–Fock Dispersion (HFD) Model as a Practical Tool for Probing Intermolecular Potentials of Small Aromatic Clusters: Comparison of the HFD and MP2 Intermolecular Potentials. *J. Phys. Chem. A* **2003,** *107*, 10105–10110.

(10) (a) Antony, J.; Grimme, S. Density Functional Theory Including Dispersion Corrections for Intermolecular Interactions in a Large Benchmark Set of Biologically Relevant Molecules. *Phys. Chem. Chem. Phys.* **2006,** *8*, 5287–5293. (b) Grimme, S.; Antony, J.; Schwabe, T.; Muck-Lichtenfeld, C. Density Functional Theory with Dispersion Corrections for Supramolecular Structures, Aggregates, and Complexes of (Bio)Organic Molecules. *Org. Biomol. Chem.* **2007,** *5*, 741–758. (c) Grimme, S.; Antony, J.; Ehrlich, S.; Krieg, H. A Consistent and Accurate Ab Initio Parametrization of Density Functional Dispersion Correction (DFT-D) for the 94 Elements H–Pu. *J. Chem. Phys.* **2010,** *132*, 19.

(11) Elstner, M.; Hobza, P.; Frauenheim, T.; Suhai, S.; Kaxiras, E. Hydrogen Bonding and Stacking Interactions of Nucleic Acid Base Pairs: A Density-Functional-Theory Based Treatment. *J. Chem. Phys.* **2001,** *114*, 5149–5155.

(12) Ortmann, F.; Bechstedt, F.; Schmidt, W. G. Semiempirical van der Waals Correction to the Density Functional Description of Solids and Molecular Structures. *Phys. Rev. B* **2006,** *73*, 205101.

(13) Liu, Y.; Goddard, W. A. A Universal Damping Function for Empirical Dispersion Correction on Density Functional Theory. *Mater. Trans.* **2009,** *50*, 1664–1670.

(14) Perdew, J. P.; Burke, K.; Ernzerhof, M. Generalized Gradient Approximation Made Simple. *Phys. Rev. Lett.* **1996,** *77*, 3865–3868.

(15) Becke, A. D. Density-Functional Thermochemistry 3. The Role of Exact Exchange. *J. Chem. Phys.* **1993,** *98*, 5648–5652.

(16) (a) Kohn, W.; Meir, Y.; Makarov, D. E. Van der Waals Energies in Density Functional Theory. *Phys. Rev. Lett.* **1998,** *80*, 4153–4156. (b) Hesselmann, A.; Jansen, G. Intermolecular Dispersion Energies from Time-Dependent Density Functional Theory. *Chem. Phys. Lett.* **2003,** *367*, 778–784.

(17) Zhang, Y.; Xu, X.; Goddard, W. A. Doubly Hybrid Density Functional for Accurate Descriptions of Nonbond Interactions, Thermochemistry, and Thermochemical Kinetics. *Proc. Natl. Acad. Sci. U.S.A.* **2009,** *106*, 4963–4968.

(18) (a) Zhao, Y.; Truhlar, D. G. How Well Can New-Generation Density Functional Methods Describe Stacking Interactions

in Biological Systems? *Phys. Chem. Chem. Phys.* **2005,** *7*, 2701–2705. (b) Xu, X.; Goddard, W. A. The X3LYP Extended Density Functional for Accurate Descriptions of Nonbond Interactions, Spin States, and Thermochemical Properties. *Proc. Natl. Acad. Sci. U.S.A.* **2004,** *101*, 2673–2677. (c) Becke, A. D.; Johnson, E. R. A Unified Density-Functional Treatment of Dynamical, Nondynamical, and Dispersion Correlations. *J. Chem. Phys.* **2007,** *127*, 124108.

(19) (a) Dion, M.; Rydberg, H.; Schroder, E.; Langreth, D. C.; Lundqvist, B. I. Van der Waals Density Functional for General Geometries. *Phys. Rev. Lett.* **2004,** *92*, 246401. (b) Puzder, A.; Dion, M.; Langreth, D. C. Binding Energies in Benzene Dimers: Nonlocal Density Functional Calculations. *J. Chem. Phys.* **2006,** *124*, 164105. (c) von Lilienfeld, O. A.; Tavernelli, I.; Rothlisberger, U.; Sebastiani, D. Optimization of Effective Atom Centered Potentials for London Dispersion Forces in Density Functional Theory. *Phys. Rev. Lett.* **2004,** *93*, 153004. (d) Tkatchenko, A.; von Lilienfeld, O. A. Adsorption of Ar on Graphite using London Dispersion Forces Corrected Kohn–Sham Density Functional Theory. *Phys. Rev. B* **2006,** *73*, 153406.

(20) Szabo, A.; Ostlund, N. S. *Modern Quantum Chemistry: Introduction to Advanced Electronic Structure Theory*; McGraw-Hill: New York, 1989.

(21) *Jaguar, 7.0*; Schrodinger, LLC: New York, 2007.

(22) Buehler, M. J.; van Duin, A. C. T.; Goddard, W. A. Multiparadigm Modeling of Dynamical Crack Propagation in Silicon using a Reactive Force Field. *Phys. Rev. Lett.* **2006,** *96*, 95505.

(23) Bailey, A. C.; Yates, B. Anisotropic Thermal Expansion of Pyrolytic Graphite at Low Temperatures. *J. Appl. Phys.* **1970,** *41*, 5088.

(24) Donohue, J. *The Structures of the Elements*; Robert E. Krieger Publishing Co.: Malabar, FL, 1974.

(25) Schultz, P. *SeqQuest, 2.58*; Sandia National Laboratory; http://www.cs.sandia.gov/~paschul/Quest/ (2004).

(26) Delhaés, P. *Graphite and Precursors*; Gordon and Breach Science: Amsterdam, The Netherlands, 2001.

(27) (a) Mayo, S. L.; Olafson, B. D.; Goddard, W. A. Dreiding — A Generic Force-Field for Molecular Simulations. *J. Phys. Chem.* **1990,** *94*, 8897–8909. (b) *BIOGRAF Program, 330*; Molecular Simulations Inc.: Burlington, MA, 1993.

(28) Benedict, L. X.; Chopra, N. G.; Cohen, M. L.; Zettl, A.; Louie, S. G.; Crespi, V. H. Microscopic Determination of the Interlayer Binding Energy in Graphite. *Chem. Phys. Lett.* **1998,** *286*, 490–496.

(29) Girifalco, L. A.; Lad, R. A. Energy of Cohesion, Compressibility, and the Potential Energy Functions of the Graphite System. *J. Chem. Phys.* **1956,** *25*, 693–697.

(30) Zacharia, R.; Ulbricht, H.; Hertel, T. Interlayer Cohesive Energy of Graphite from Thermal Desorption of Polyaromatic Hydrocarbons. *Phys. Rev. B* **2004,** *69*, 155406.

(31) Spanu, L.; Sorella, S.; Galli, G. Nature and Strength of Interlayer Binding in Graphite. *Phys. Rev. Lett.* **2009,** *103*, 196401.

(32) Rydberg, H.; Jacobson, N.; Hyldgaard, P.; Simak, S. I.; Lundqvist, B. I.; Langreth, D. C. Hard Numbers on Soft Matter. *Surf. Sci.* **2003,** *532*, 606–610.

DOI: 10.1021/jz100615g | *J. Phys. Chem. Lett.* **2010,** *1*, 2550–2555